γ

PNL-SA-18461

CONF-9008178--1

PNL-SA--18461

DE91 005704

Received by OSTI

JAN 04 1991

VARIATIONAL TRANSITION STATE THEORY CALCULATIONS OF TUNNELING EFFECTS ON CONCERTED HYDROGEN MOTION IN WATER CLUSTERS AND FORMALDEHYDE/WATER CLUSTERS

August 1990

B. C. Garrett
C. F. Melius

Presented at the
North Atlantic Treaty Organization
Advanced Studies Institiute on
Theoretical and Computational Models
for Organic Chemistry
Porto Novo Beach, Vimeiro, Portugal
August 26-September 8, 1990

Work supported by the
U. S. Department of Energy
under Contract DE-AC06-76RLO 1830

MASTER

DISTRIBUTION OF THIS DOCUMENT IS UNLIMITED

Pacific Northwest Laboratory
Richland, Washington 99352

Contribution to the book of proceeding for the NATO Advanced Studies Institute on Theoretical and Computational Models for Organic Chemistry, August 26 - September 8, 1990, Porto Novo Beach, Vimeiro, Portugal

VARIATIONAL TRANSITION STATE THEORY CALCULATIONS OF CONCERTED HYDROGEN ATOM TUNNELING IN WATER CLUSTERS AND FORMALDEHYDE/WATER CLUSTERS

Bruce C. Garrett
Molecular Science Research Center
Pacific Northwest Laboratory*
Richland, WA 99352

Carl F. Melius
Sandia National Laboratories
Livermore, CA 94550

ABSTRACT. The direct participation of water molecules in aqueous phase reaction processes has been postulated to occur via both single-step mechanisms as well as concerted hydrogen atom or proton shifts. In the present work, simple prototypes of concerted hydrogen atom transfer processes are examined for small hydrogen-bonded water clusters – cyclic trimers and tetramers – and hydrogen-bonded clusters of formaldehyde with one and two water molecules. Rate constants for the rearrangement processes are computed using variational transition state theory, accounting for quantum mechanical tunneling effects by semiclassical ground-state adiabatic transmission coefficients. The variational transition state theory calculations directly utilize selected information about the potential energy surface along the minimum energy path as parameters of the reaction path Hamiltonian. The potential energy information is obtained from *ab initio* electronic structure calculations with an empirical bond additivity correction (the BAC-MP4 method). Tunneling is found to be very important for these concerted rearrangement processes – the semiclassical ground-state adiabatic transmission coefficients are estimated to be as high as four orders of magnitude at room temperature. Effects of the size of the cluster (number of water molecules in the cyclic complex) are also dramatic – addition of a water molecule is seen to change the calculated rates by orders of magnitude.

1. Introduction

Hydrogen atom and proton transfer are among the simplest of elementary processes that can occur in aqueous solutions. These processes are important in proton transfers in enzyme and other biochemical processes, chemical reactions occurring in aqueous solutions, and oxidation of organic waste in supercritical aqueous solutions. Large proton transfer rates between oxygen atoms in organic acids have been observed in alcohol and aqueous solutions of acids, and these have been attributed to multiple proton jumps involving direct participation of solvent molecules [1-3]. Using simple models for the potential energy surfaces, the relative energetics of reaction pathways have been used to examine the competition between stepwise mechanisms and concerted processes of proton transfer [4-8]. *Ab Initio* electronic structure methods have also been employed to investigate the mechanisms of these proton transfer processes [9-11]. In some instances large measured rates for proton transfer have been attributed to concerted processes [12-14].

In this paper prototypes of concerted hydrogen atom transfer in hydrogen-bonded clusters are examined using modern computational techniques for obtaining reaction energetics and for calculating reaction rates. The effects of the size of the cyclic hydrogen-bonded cluster on calculated rates of hydrogen atom transfer processes are studied for water trimers and tetramers, diagrams 1 and 2 below, and for formaldehyde hydrolysis by one and two water molecules, diagrams 3 and 4 below. We treat the unimolecular process of reacting from the bound hydrogen-bonded cluster. In aqueous phase the breaking up and reformation of these cyclic structures will be facile and calculation of the rates of these processes in condensed phase will be more complicated. Furthermore, other mechanisms may be important, for example, it may be more realistic to treat reaction 4 as a formaldehyde molecule which is solvated and reacting with a water dimer in bulk water rather than a unimolecular rearrangement. In addition, these complexes will be solvated by water molecules that do not directly participate in the hydrogen atom transfer and this will also change the reaction energetics. These effects are beyond the scope of the current paper which represents a first step towards addressing some of these more complicated issues.

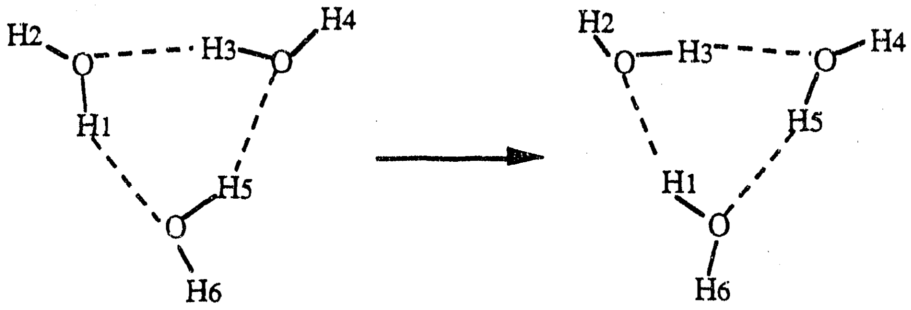

1

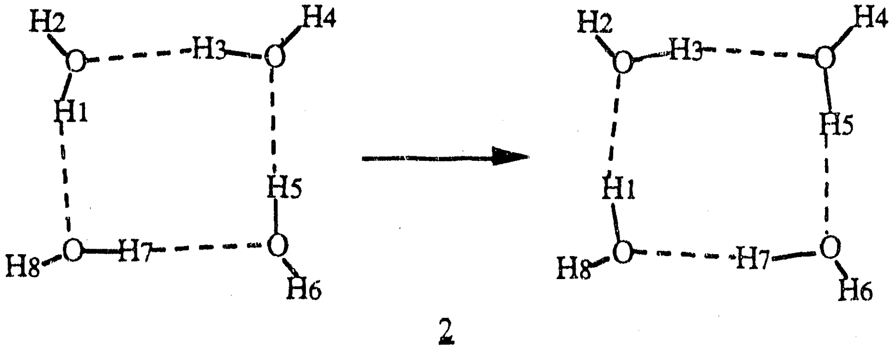

2

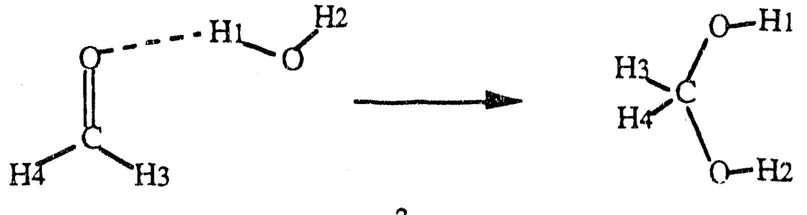

3

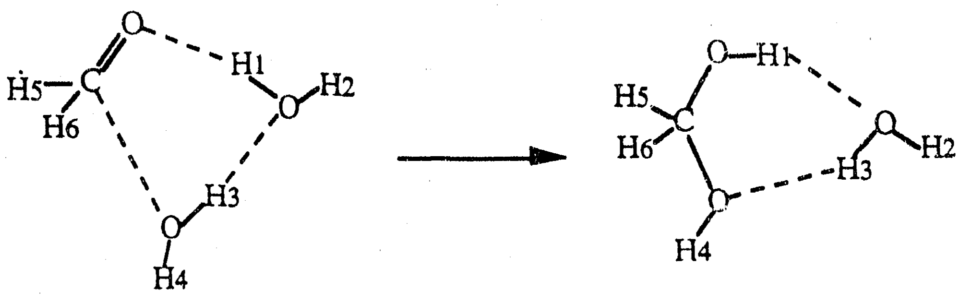

4

Rate constants for these unimolecular processes are calculated using variational transition state theory with semiclassical adiabatic ground-state transmission coefficients [15-25]. These calculations include important quantum mechanical tunneling effects by the small-curvature semiclassical adiabatic ground-state method which includes the effects of curvature of the reaction path. Compared to conventional transition state theory [26] with simple tunneling correction factors based on quadratic expansions of the potential energy surface near the saddle point [27], variational transition state theory with semiclassical adiabatic ground-state transmission coefficients uses a more extended description of the potential along a reaction path and is able to provide more quantitative predictions of reaction rates. Even though variational transition state theory requires more extensive descriptions of the potential energy surface, these calculations can directly utilize potential information obtained from modern electronic structure methods, i.e., the energy and derivatives of the energy along a reaction path, providing an efficient means of estimating reaction rates from first principles calculations [15].

In the present work, information about the potential energy surfaces for these systems is obtained by the BAC-MP4 method [28-33]. This method has been very successful for predicting the thermochemistry of molecules and radical species, and has been extended to calculating the potential information along reaction paths needed for the variational transition state theory calculations. In the latter case, the method has been shown to be capable of quantitative predictions for a gas phase chemical reaction [33]. In the present study our interests are in estimates of the order of magnitude of reaction rates, and in studies of qualitative trends such as the effect of cluster size on the magnitude of quantum tunneling. The methods employed here are more than adequate for these types of studies.

The previous studies of concerted hydrogen atom and proton transfer in hydrogen-bonded systems have been limited to studies of reaction pathways for simple model systems [4-8] with simple, reduced dimensionality methods for including quantum tunneling [13,14,34,35]. The applicability of modern computational methods to such systems is exemplified by more recent studies of the energetics of intramolecular hydrogen atom transfer in molecules such as malonaldehyde [36-39] and models of tunneling in malonaldehyde [39,40]. Williams and coworkers [10] have used *ab initio* electronic structure methods to investigate the concerted proton transfer reaction mechanism in addition to carbonyl groups. We extend the studies of Williams *et al.* to include higher levels of electron correlation and follow the entire reaction pathway in order to apply variational transition state theory and to treat the tunneling process.

Variational transition state theory, including semiclassical transmission coefficients, has been extensively review in the literature [15-25], and the use of variational transition state theory with the BAC-MP4 method has also been described in detail [33]. The reader is referred to the previous papers for details of the theory and the computational procedures; a brief outline of the

Hartree-Fock level with the 6-31G* basis. We then distinguish the method for computing the energy along the reaction path as HF, MP4 (which is computed with the 6-31G** basis), and BAC-MP4 when the bond-additivity correction is added to the MP4 results.

The bond additivity correction is typically computed only for atom pairs with interatomic distances within a preset cutoff. For studying chemical reactions in which bonds are made and broken it is necessary to force the BAC to be computed for some pairs of atoms at all distances to insure continuity of potential energy curves. In the present study the BAC is applied to all the hydrogen-bonded interactions, although in the standard application it is not. This introduces approximately an additional 0.8 kcal/mol of binding for each hydrogen-bonded interaction at the equilibrium hydrogen-bonded internuclear distance.

Rate constant calculations were carried out using the POLYRATE program [23]. These calculations directly utilize the energy and the first and second derivatives along the minimum energy path. Rate constants are calculated by the canonical variational theory (CVT) [24] with multidimensional quantum mechanical tunneling effects included by the small-curvature semiclassical adiabatic ground-state (SCSAG) transmission coefficient [46,47]. The small-curvature semiclassical adiabatic ground state (SCSAG) method includes the effect of the reaction-path curvature to induce the tunneling path to 'cut the corner' and shorten the tunneling length. A central quantity in both the CVT and SCSAG calculations is the ground-state adiabatic potential curve

$$V_a^G(s) = V_{MEP}(s) + \sum_{m=1}^{F-1} \varepsilon_{vib,m}^{GT}(n_m=0,s) \tag{1}$$

where $V_{MEP}(s)$ is the value of the potential along the reaction path at s, the sum is over the F-1 bound vibrational modes of the generalized transition state at s (F=3N-6, where N is the number of atoms), and $\varepsilon_{vib,m}^{GT}(n_m,s)$ is the bound energy level for state n_m in mode m at the generalized transition state. It is also useful to define the adiabatic potential relative to the total zero-point energy of the reactants

$$\Delta V_a^G(s) = V_a^G(s) - \sum_{m=1}^{F} \varepsilon_m^R(n_m=0) \tag{2}$$

where $\varepsilon_m^R(n_m)$ is the reactant energy level for state n_m in mode m and the sum goes over F bound modes (instead of the F-1 modes at the generalized transition state where the reaction coordinate motion is the Fth mode). Choosing the zero of energy such that $V_{MEP}(s)$ is zero at the reactant equilibrium geometry, the maximum of $\Delta V_a^G(s)$ is the adiabatic threshold for reaction. In the current studies we treat all bound degrees of freedom harmonically, and the energy levels are given simply by

$$\varepsilon_{vib,m}^{GT}(n_m,s) = (n_m+\tfrac{1}{2})\hbar\omega_m(s) \tag{3}$$

where $\omega_m(s)$ is the harmonic frequency for mode m at the generalized transition state located at s. The harmonic frequencies are obtained from the gradient vector and Hessian matrix using the projection technique of Miller, Handy, and Adams [48].

More accurate calculations of the reaction rates require a careful investigation of the effects of anharmonicity, especially for the the low frequency modes in these loosely bound complexes. As discussed elsewhere [33], effects of anharmonicity are approximately included in the empirical BAC correction. A manifestation of anharmonicity in these hydrogen-bonded complexes is multiple minima in the equilibrium region and multiple transition states that correspond to different orientations of the terminal hydrogens in these cyclic complexes. For example, in the cyclic water trimer, orienting the three hydrogens labeled H2, H4, and H6 in diagram 1 below the plane of the 6-atom ring is slightly higher in energy than to have two hydrogens below and one above the plane. These two minima are similar in energy – they differ by about two kcal/mol – and are separated by a transition state of less than a kcal/mol. Similarly, in the transition state region for the reaction in diagram 1, the two transition structures with all terminal hydrogens below the plane is higher in energy by about two kcal/mol than for two below and one above the plane. The harmonic approximation for these H wagging modes will underestimate the contribution to the partition functions for these modes. However, since these modes are treated the same in the reactant and transition state, the errors will tend to cancel.

Another concern in the dynamical calculations is the accuracy of the approximations used in the calculations of the quantum tunneling corrections. The concerted processes considered here are light hydrogen atom transfers between heavy groups. In analogy with gas phase reactions of light atom transfer between two heavy moieties, these types of systems have regions of the reaction path with high reaction-path curvature. For reactions in which tunneling occurs in regions of high reaction-path curvature, the SCSAG method only gives qualitative estimates of the tunneling factor; more reliable estimates can be obtained using the large-curvature ground-state (LCG) method [22,49] which has recently been extended to polyatomic systems [50]. However, in its present implementation, it can only be applied with global potential energy surfaces, although there are indications that the method can be adapted to using only limited information about the potential energy surface within the framework of the reaction path Hamiltonian [50].

The transmission coefficients are obtained from Boltzmann averages of the probabilities for tunneling through the ground-state adiabatic barrier. For the unimolecular processes considered here the reactant and product species correspond to local wells in the adiabatic potential separated by the adiabatic barrier. For this case, averaging over a continuum of translational energies is only an approximation since tunneling occurs from discrete energy levels in the bound wells of the adiabatic potential [51,52]. For the systems studied in this paper, the barriers are high and the adiabatic potentials will support many states. Thus, the continuum limit will yield a reasonable approximation. Quantitative accuracy in calculations of reaction rates for polyatomic systems presents a challenge because of limited accuracy in the computed energies and the approximations in the dynamical calculations of the rates. However, the methods used here will provide good estimates of the orders of magnitude for these reactions and will be very useful for predicting relative rates in homologous series of reactions.

3. Results and Discussion

3.1. STRUCTURE AND ENERGETICS OF WATER CLUSTERS

The heat of formation of water at 0 K using the BAC-MP4 method is taken to be -57.1 kcal/mol, the same as the experimental value [53]. The accuracy of the BAC-MP4 method for predicting the structure and binding in hydrogen-bonded clusters is tested by comparing the calculated values with experiment [54,55] and with previous calculations [56,57]. The calculated geometry is shown in diagram 5 (bond lengths are in units of Å).

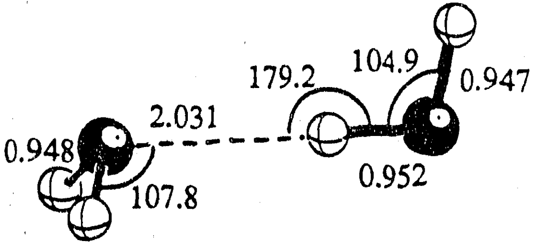

5

The bond angles and lengths are in reasonable agreement with previously calculated results. The computed hydrogen-bond energy (neglecting zero-point energy) in the dimer is 5.5, 6.7, and 7.4 kcal/mol computed by the HF, MP4, and BAC-MP4 levels of theory. The heat of formation of the dimer from two water molecules at 0 K is computed to be -5.2 kcal/mol at the BAC-MP4 level. This is about 2 kcal/mol lower in energy than the experimental value and is consistent with the reliability of the BAC-MP4 method.

The lowest energy equilibrium cyclic configuration of the trimer is shown in diagram 6. This agrees with previous *ab initio* electronic structure calculations [58,59]. The $(OH)_3$ ring is nearly planar – the largest distortion out of plane is about 9° – and two of the terminal H atoms are below the plane with one above. The hydrogen bonds are not quite symmetric – bond lengths range from 1.99 to 2.01 Å – and the OHO bond angle varies from 150° to 152°. Relative to three separated water molecules (at their equilibrium geometries), the cyclic trimer is calculated to be bound by -17.1, -21.5, and -23.6 kcal/mol at the HF, MP4, and BAC-MP4 levels of theory (these energies represent the electronic energies without zero-point energies), and the heat of formation relative to three water molecules is predicted by the BAC-MP4 method to be -17.7 kcal/mol at 0 K.

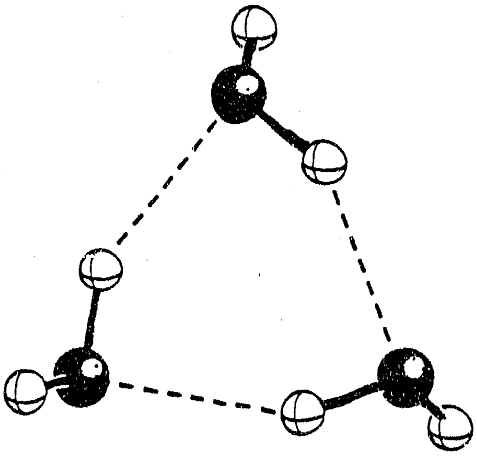

6

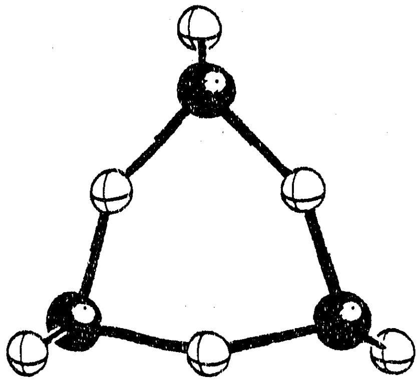

7

The rearrangement of the hydrogens as indicated in diagram 1 proceeds via the transition state structure shown in diagram 7. The transition state is also nearly planar – its largest out-of-plane distortion is about 10°. The ring OH bonds are all 1.21 Å and the OHO bond angles are all 153°. The OO distances in the transition state structure are about 2.3 Å which is smaller than the values of 2.9 Å in the equilibrium geometry. The energy of the transition state structure is predicted to be higher than that of the equilibrium structure 6 by 46.6, 28.8, and 29.1 kcal/mol at the HF, MP4, and BAC-MP4 levels of theory. Although the HF calculations give hydrogen-bond energies that differ from the higher quality MP4 calculation by only about 2 kcal/mol for each hydrogen bond, the energy of the transition state for the bond-breaking and bond-making process is nearly 18 kcal/mol higher at the HF level than the MP4 level.

Frequencies calculated as a function of location along the reaction path are presented in figure 1. The highest frequency modes corresponds the the OH stretch for the terminal hydrogens. These frequencies change only slightly as a function of the reaction coordinate. The next (lower) set of frequencies correlate with the 'in-plane' OH stretch in the equilibrium configurations. At the saddle point the OH bond is stretched relative to the equilibrium geometries and this frequency is greatly reduced.

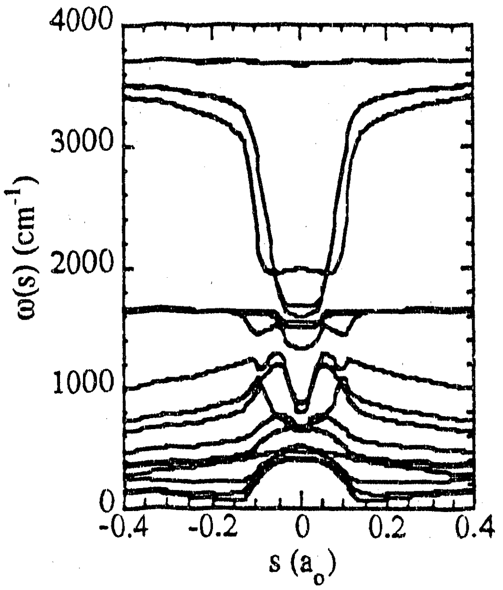

Figure 1. Harmonic frequencies for bound modes orthogonal to the reaction path as a function of the reaction coordinate for the concerted hydrogen atom transfer in the water trimer (see diagram 1).

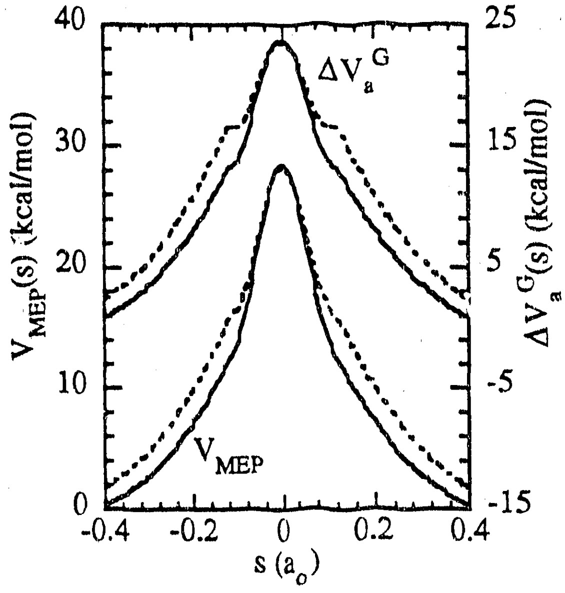

Figure 2. Potential energy along the minimum energy path and relative ground-state adiabatic potential energy [eq. (2)] as a function of reaction coordinate for the concerted hydrogen atom transfer in the water trimer. The zero of energy for the potential along the minimum energy path is the at the equilibrium geometry of the reactants. Solid lines are calculated using the BAC-MP4 calculations and the dashed curves are computed using the MP4 calculations.

Rapid changes in the frequencies occur near $s=\pm0.1\ a_0$ which is the region of the reaction path with the highest reaction path curvature. Near the saddle point, the reaction coordinate motion corresponds mostly to concerted motion of the three hydrogen atoms in the ring and this motion occurs along nearly straight lines in cartesian coordinates. However, as is evident from diagrams 6 and 7 the oxygen atoms must also move away from each other in proceeding along the reaction coordinate from the saddle point to the equilibrium geometry. Near $s=\pm0.1$ a_0 the reaction coordinate motion incorporates more oxygen atom motion and the coupling of the oxygen and hydrogen motions along the reaction path leads to more reaction-path curvature.

The energy on the minimum energy path (neglecting zero-point energy effects) $V_{MEP}(s)$ and the ground-state adiabatic potential curve relative to the reactant zero point energy $\Delta V_a^G(s)$ are plotted in figure 2. The BAC-MP4 (solid curves) and MP4 energies (dashed curves) agree surprisingly well, indicating that the bond additivity correction nearly cancels out between reactants and points along the reaction path. Besides the large drop in the three 'in plane' OH stretches in going from the reactants to the saddle point, as indicated above, there is one extra bound vibrational mode in reactants that becomes the unbound reaction coordinate motion at the saddle point: This is the mode which contributes to the zero-point energy of the reactants, but has no contribution to the adiabatic potential along the reaction coordinate. Thus, the zero-point energy at the saddle point is nearly 5 kcal/mol lower than at the reactants, leading to an adiabatic threshold of only 24 kcal/mol compared to the classical barrier height of about 28 kcal/mol.

Diagrams 8 and 9 show the lowest energy cyclic configuration of the water tetramer and the transition state for the rearrangement process depicted in diagram 2. As for the cyclic trimer, the lowest energy equilibrium geometry of the cyclic tetramer also has a nearly planar $(OH)_4$ ring – the largest out-of-plane distortion is 20°. The terminal hydrogens alternate above and below the plane of the ring. The OHO bond angles in the tetramer are about 167°, which is closer to the preferred near collinear geometry than for the trimer, and the hydrogen-bond lengths are all near 1.88 Å. Relative to four separated water molecules, the cyclic tetramer is lower in energy by -29.0, -35.9, and -39.2 kcal/mol by the HF, MP4, and BAC-MP4 methods, and the BAC-MP4 predicts the heat of formation from the water molecules to be 30.4 kcal/mol at 0 K.

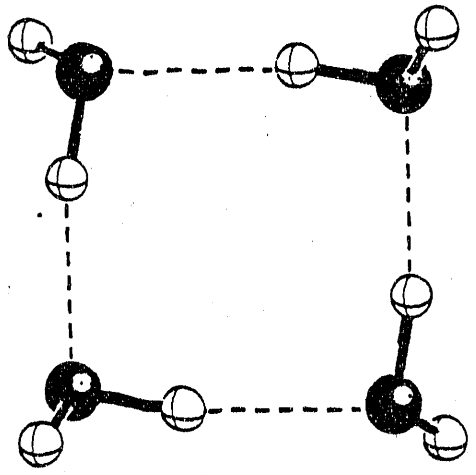

8

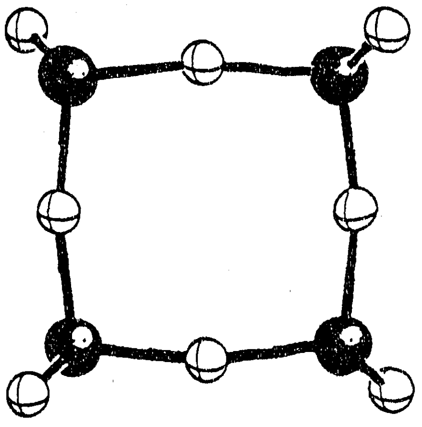

9

The transition state structure has a planar ring – its largest distortion is only 2°. The OHO bond angles are 168°, very closer to those for the equilibrium structure, and all the OH bond lengths in the ring are 1.20 Å. Similar to the trimer structures, the OO distances change from 2.8 Å in the equilibrium structure to 2.4 Å in the transition state structure. Relative to the reactant complex, the transition state is higher in energy by 45.2, 25.0, and 25.1 kcal/mol at the HF, MP4, and BAC-MP4 methods. As was the case for the water trimer, the HF method is much higher in energy than the MP4 method, but the MP4 and BAC-MP4 methods agree very well.

Frequencies and potential energy curves for the concerted hydrogen atom transfer process in the tetramer (diagram 2) are presented in figures 3 and 4. The variations of the frequencies with s are very similar to those for the trimer; for the OH bonds in the ring, the stretching frequencies exhibit large changes in going from the reactant to the transition state. The potential curve $V_{MEP}(s)$ for the tetramer is very similar in shape to that for the trimer (shown as a dashed curve in figure 4) but the barrier height is lower in energy by about 4 kcal/mol. The changes in zero-point energies in going from the reactant to the saddle point are greater in the tetramer than the trimer. The difference in adiabatic thresholds is nearly 8 kcal/mol. The adiabatic potential for the tetramer also shows more structure and is a little broader than that for the trimer.

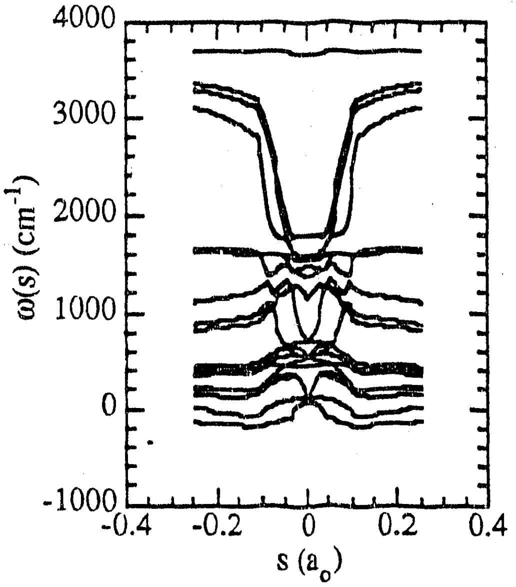

Figure 3. Same as figure 1 except for the concerted hydrogen atom transfer in the water tetramer (see diagram 2).

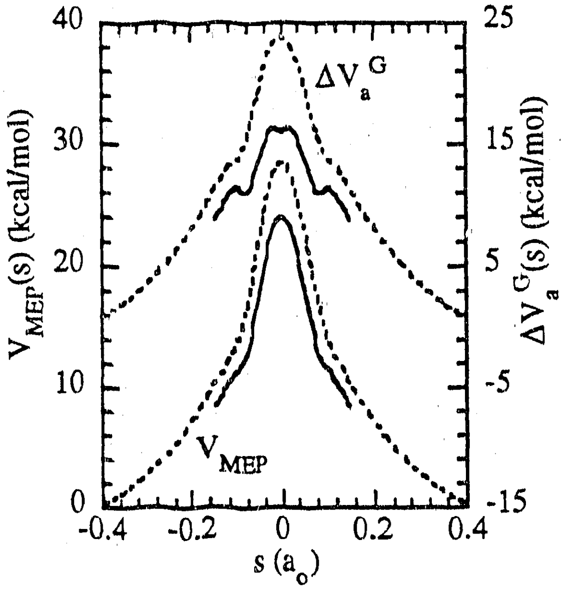

Figure 4. Comparison of potential energy along the minimum energy path and relative ground-state adiabatic potential for the concerted hydrogen atom transfer in the water trimer (dashed curves) and water tetramer (solid curves), using BAC-MP4 calculations.

3.2 STRUCTURES AND ENERGETICS OF FORMALDEHYDE-WATER CLUSTERS

Diagrams 10, 11, and 12 show the reactant, transition state, and product structures for formaldehyde hydrolysis by one water molecule (see diagram 3). The reactant complex is nearly planar for the COHO forming a 'ring' – the torsion angle for these four atoms is only 11°. The OH hydrogen bond has a length of 2.1 Å and the distance for the oxygen in the water molecule to the carbon atom is 3.2 Å. The dimer is bound relative to separated formaldehyde and water by 5.2, 6.6, and 7.3 kcal/mol by the HF, MP4 and BAC-MP4 methods. For the products, diagram 12, the CO bonds lengths are 1.4 Å with OH bond lengths of 0.95 Å. Relative to separated formaldehyde and water, the diol is more bound by 14.6, 14.2, and 17.5 kcal/mol at the HF, MP4, and BAC-MP4 levels of theory.

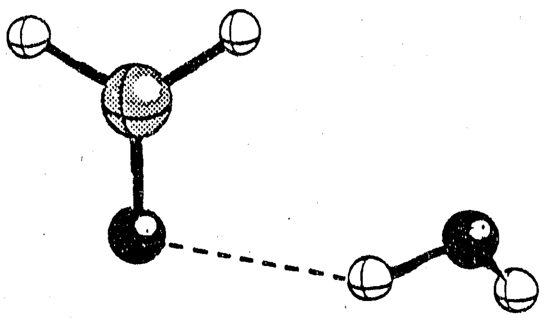

10

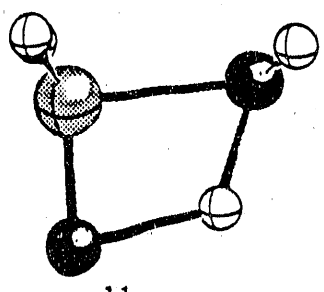

11

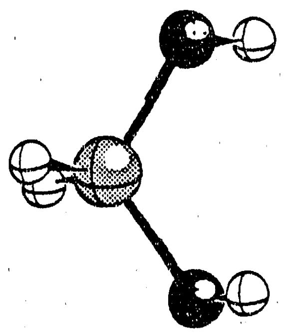

12

The transition state shown in diagram 11 is much nearer to planar than the reactant with an out-of-plane torsion of less than 0.1°. Compared to the reactants, the OH hydrogen bond has shortened to 1.3 Å, the distance from the carbon to the water oxygen is only 1.6 Å, and the 'active' OH bond in water has lengthened from 0.95 Å to 1.15 Å. The energy of the transition state relative to the reactant dimer is 53.5, 42.3, and 41.0 kcal/mol by the HF, MP4, and BAC-MP4 methods. Once again the HF method gives an energy which is much larger than either the MP4 or BAC-MP4 methods. As was the case for the water clusters, the MP4 and BAC-MP4 methods agree well for the relative energetics going from the hydrogen-bonded species to the transition state. However, the two methods do not agree as well for the overall reaction energetics (product energies relative to reactant energies) – the MP4 method predicts the reaction is downhill by 7.7 kcal/mol while the BAC-MP4 method predicts 10.2. The BAC-MP4 method has been shown to predict the heats of formation of bound species more accurately, therefore we prefer the BAC-MP4 results over the MP4 results in this case.

Plots of frequency and potential energies versus reaction coordinate are shown in figures 5 and 6. As for concerted hydrogen atom transfer in water clusters, some of the harmonic frequencies exhibit dramatic changes in going from the reactant to the saddle point. The high frequency mode which changes the most corresponds to the OH bond of the water that is being broken and will become the new OH bond in the diol. Unlike the water clusters which indicate a lower zero-point energy at the saddle point compared to the hydrogen-bonded reactant, for formaldehyde hydrolysis the adiabatic threshold and classical barrier heights agree to within 0.3 kcal/mol. Obviously the marked decrease in one high frequency mode is offset by the more gradual increase in many of the low frequency modes. The classical potential $V_{MEP}(s)$ and the relative adiabatic potential $\Delta V_a^G(s)$ are nearly identical in height and shape for this process.

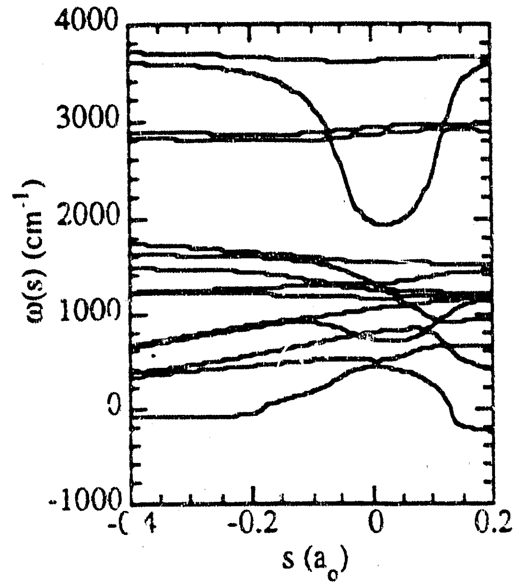

Figure 5. Same as figure 1 except for formaldehyde hydrolysis by a single water molecule (see diagram 3).

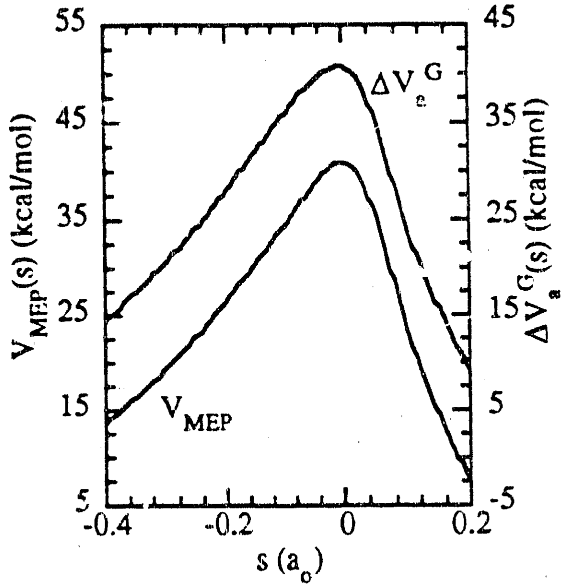

Figure 6. Potential energy along the minimum energy path and relative ground-state adiabatic potential curves as a function of reaction coordinate for formaldehyde hydrolysis, by one water, using BAC-MP4 calculations.

Diagrams 13, 14, and 15 show the reactant, transition state, and product structures for formaldehyde hydrolysis by two water molecules (see diagram 4). In the reactant complex, the OHOHO forming the ring is nearly planar – the largest out-of-plane angle is only 9° – but the carbon atom is distorted from planar by 22°. The OH hydrogen bond between the carbonyl oxygen and water has a length of 2.1 Å, the water-water OH hydrogen-bond length is 2.0 Å, and the distance for the oxygen in water to the carbon atom is 2.8 Å. The dimer is bound relative to separated formaldehyde and 2 water molecules by 13.5, 16.4, and 16.0 kcal/mol by the HF, MP4 and BAC-MP4 methods.

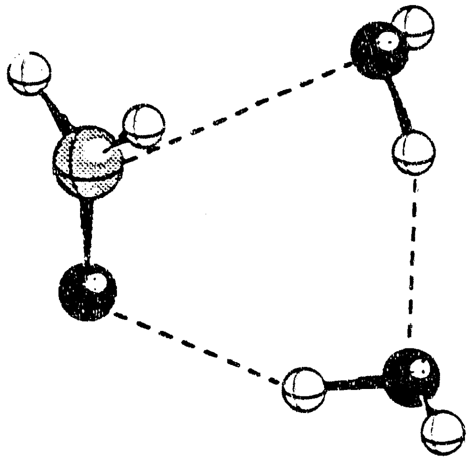

13

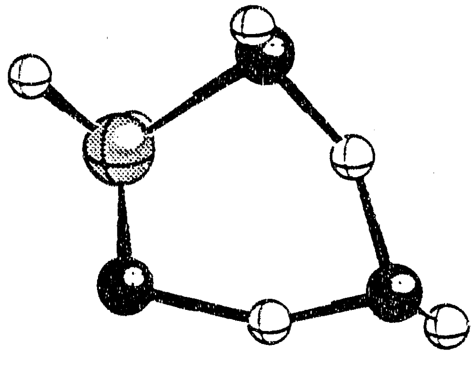

14

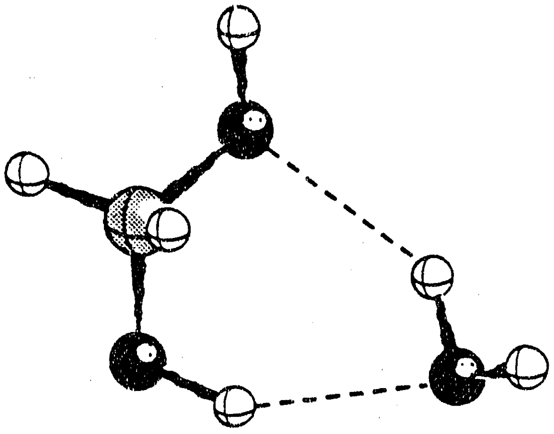

15

For the product, diagram 15, the CO bonds lengths are 1.4 Å with OH bond lengths of 0.95 Å. The OH hydrogen-bond lengths are 2.0 Å for the distance from the water O to alcohol H, and 2.1 Å for the distance from the alcohol O to the water H. The OH groups that help form the ring are nearly planar – the largest torsion angle is only 5° – but the two CO bonds are at angles of 21° and 38° to this plane. Relative to separated formaldehyde and two water molecules, the diol-water complex is more bound by 18.6, 20.7 and 23.7 kcal/mol at the HF, MP4, and BAC-MP4 levels of theory.

For the transition state shown in diagram 14, the atoms OHOHO that form the ring with C is much nearer to planar than the reactant – the largest out-of-plane torsion is about 5° – but the carbon atom is still out of the plane – the largest out-of-plane torsion is about 30°. All OH bonds in the ring are intermediate between a covalent OH bond length of 0.95Å and a hydrogen-bond OH bond length of nearly 2.0 Å. The distance from the carbon atom to oxygen atom in the water molecule is 1.6 Å and the carbonyl CO bond length has lengthened from 1.2 Å to 1.3 Å. The energy of the transition state relative to the reactant dimer is 40.1, 24.2, and 20.3 kcal/mol by the HF, MP4, and BAC-MP4 methods. Once again the HF method gives an energy which is much larger than either the MP4 or BAC-MP4 methods. As for the water clusters, the MP4 and BAC-MP4 methods agree well for the relative energetics going from the hydrogen-bonded species to the transition state. However, the two methods do not agree as well for the overall reaction energetics (product energies relative to reactant energies) – the MP4 method predicts the reaction is downhill by 4.3 kcal/mol while the BAC-MP4 method predicts 7.7 kcal/mol.

The frequencies as a function of reaction coordinate presented in figure 7 show the same general behavior seen for the formaldehyde-water cluster. As in the previous case, the zero-point energy of the reactant is within 0.3 kcal/mol of the zero-point energy of the reactants. Therefore, the relative adiabatic potential at the saddle point is nearly equal to the classical barrier height. As seen in figure 8, the maximum of the adiabatic potential occurs about 0.06 a_0 before the barrier and is about 1.3 kcal/mol higher than the value at the saddle point. Compared to the formaldehyde-single-water reaction, the classical barrier for the reaction with two water molecules is lowered by over 20 kcal/mol and the adiabatic threshold is lowered by 17.5 kcal/mol. The shapes of the two classical barriers are very similar for the two systems, but the adiabatic barrier for the system with two waters is slightly broader than that for the single water system.

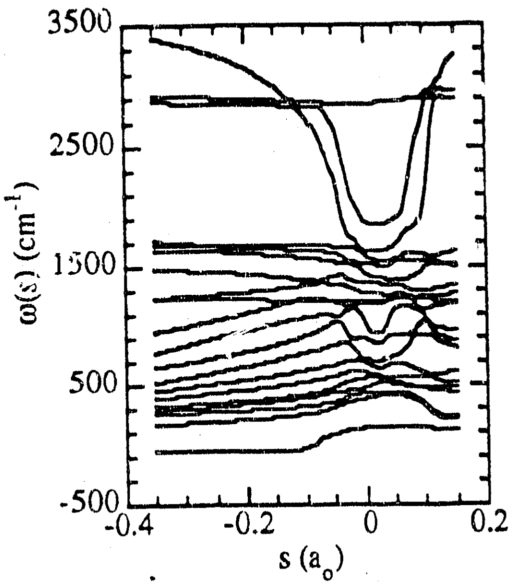

Figure 7. Same as figure 1 except for formaldehyde hydrolysis by two water molecules (see diagram 4).

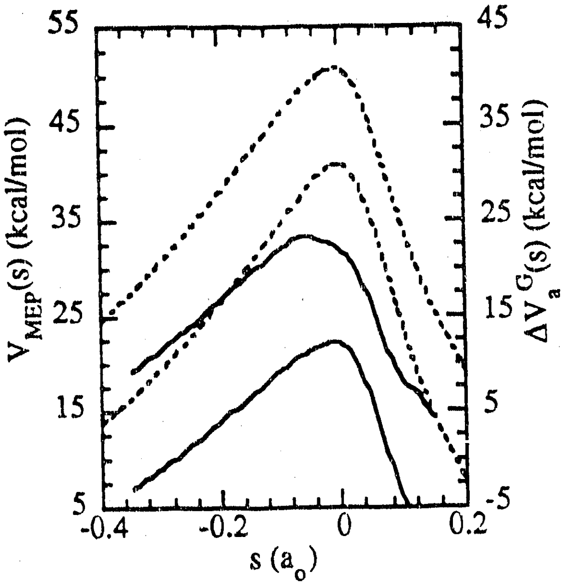

Figure 8. Comparison of potential energy along the minimum energy path and relative ground-state adiabatic potential as a function of reaction coordinate for formaldehyde hydrolysis by one water molecule (dashed curves) and two water molecules (solid curves), by BAC-MP4 calculations. For each set, the top curve is the the adiabatic potential to lower curve is the potential energy.

3.3 REACTION RATES

In this paper, the direct participation of water molecules in the concerted proton transfer process has been addressed, but the large solvating effect of surrounding water molecules on the stabilization of the transition state has not been considered. For the reactions studied here, the barriers are quite high, ranging from ~16 kcal/mol to ~40 kcal/mol. As a consequence, the resulting gas-phase rate constants are quite low and would not be measurable in the temperature range from room temperature up to about 600 K. However, it is interesting to see how these rates vary with the number of participating water molecules in the concerted proton transfer and how the number of participating water molecules effects the importance of tunneling. Rates for the hydrogen atom transfer processes in water clusters (diagrams 1 and 2) are shown in figure 9 and those for the two formaldehyde hydrolysis reactions (diagrams 3 and 4) are compared in figure 10.

The rate constants for the concerted hydrogen atom transfer in cyclic water clusters are seen to change dramatically with the number of waters in the clusters. The CVT/SCSAG rate constants for the tetramer are enhanced by factors of 4.5×10^4, 7500, and 4 relative to the trimer for temperatures of 200, 300, and 400 K. Tunneling is very important for these reactions, as can be seen by comparing the CVT results (which neglects tunneling) with the CVT/SCSAG results in figure 9. Tunneling is more important for the trimer – with tunneling correction factors of 1.7×10^5, 42, and 5 at 200, 300, and 400 K – than for the tetramer – with tunneling corrections factors of 280, 5.4, and 2.1 for the same temperatures. As is seen in figure 4, the adiabatic barrier is broader for the tetramer and the reduced mass factor for the tetramer is larger. Both factors contribute to the diminished tunneling.

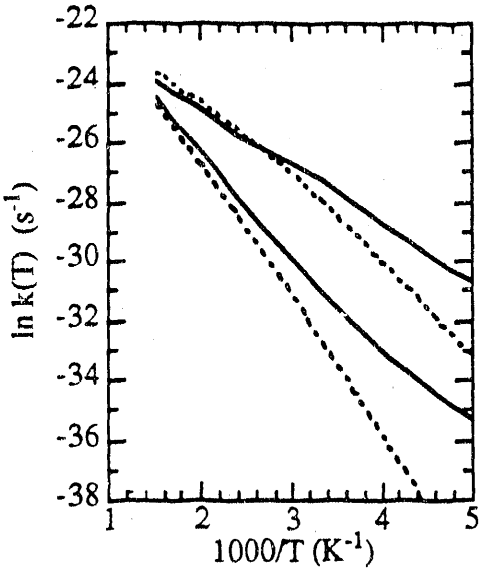

Figure 9. Rate constants calculated by the CVT (dashed curves) and CVT/SCSAG (solid curves) methods for concerted hydrogen atom transfer in cyclic water trimers (lower set of curves) and tetramers (upper set of curves).

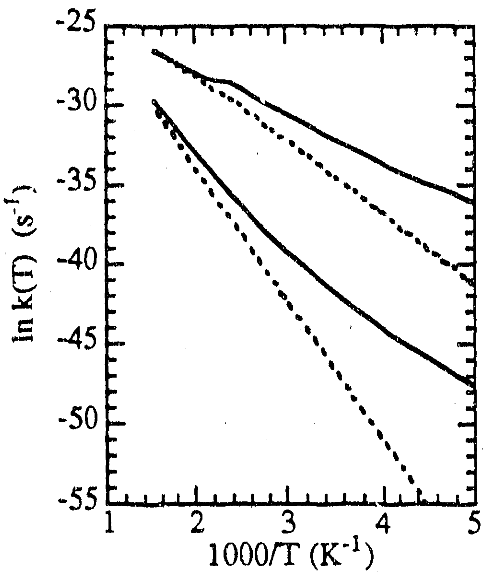

Figure 10. Same as figure 9 except for formaldehyde hydrolysis by one water molecule (lower set of curves) and by two water molecules (upper set of curves).

The changes in the rate constants with addition of water molecules are even larger for formaldehyde hydrolysis. Compared to the reaction with one water molecule, the rates of the reaction with two water molecules are enhanced by 3.4×10^{11}, 2.1×10^{9}, and 2.2×10^{7} at 200, 300, and 400 K. Tunneling is also important for formaldehyde hydrolysis: the tunneling correction factors are 6.1×10^{11}, 1.6×10^{4}, and 77 with one water, and 12, 2.5, and 1.6 for two waters at 200, 300, and 400 K. As for the concerted hydrogen atom transfer in the water clusters, the broader adiabatic barrier and heavier reduced mass diminish the tunneling in the larger cluster.

In an aqueous environment, the surrounding medium of additional water molecules will further stabilized the transition state structure of the proton transfer reaction through hydrogen bonding. This solvation stabilization is greater for the transition state than for the reactants due to the greater ionic character of the transition state. Using an equation of state with critical parameters scaled from changes in the atomic charge of each hydrogen [60], we estimate that the free energy of activation for the reaction in diagram 2 is lowered by 18.3 kcal/mol. This large lowering of the activation barrier will significantly flatten the adiabatic potential along the reaction coordinate, thereby decreasing the effect of tunneling significantly. On the other hand, the overall rate constant will be greatly increased due to the lower adiabatic activation energy. Thus, we expect the effect of increasing the polar strength of the solvent will be to decrease the tunneling contribution to the rate constant, but increase the proton transfer rate. More reliable estimates of the rates of these processes in aqueous solutions will also require calculations of the equilibrium populations of these cyclic complexes in solution. One expects the population of the complexes to decrease with increase in the number of water molecules in the complex; therefore, even though the rates of reaction are larger for the larger complexes, they may be less important in the overall mechanism. The calculations of the rates presented here will be of more direct relevance to these clusters in aprotic, yet polarizable, solvents. We are pursuing further research on the effects of the solvating medium on the concerted proton transfer reaction within the variational transition state theory formalism.

4. Conclusions

Rate constants have been computed over a temperature range from 200 to 600 K for the concerted hydrogen atom transfer in cyclic water trimer and tetramer, and for formaldehyde hydrolysis in clusters with one and two water molecules. The rates are computed by variational transition state theory with semiclassical adiabatic ground-state transmission coefficients using limited information about the potential energy surface along the reaction path. This type of information about the potential is obtained directly from *ab initio* electronic structure calculations of the energy and its first and second derivative with respect to coordinates. In the present calculations, *ab initio* information is empirically adjusted by the BAC-MP4 method to yield more reliable predictions of the reaction energetics.

Dramatic effects of the number of participating water molecules on the reaction rates are predicted. At 300 K, enhancements of nearly four orders of magnitude and over nine overs of magnitude are obtained for the addition of a water molecule to the cyclic water trimer and the formaldehyde water dimer, respectively. Tunneling is also predicted to be important for these systems but the effect diminishes as additional water molecules participate actively in the proton transfer.

References

* Pacific Northwest Laboratory is operated for the U. S. Department of Energy by Battelle Memorial Institute under contract DE-AC06-76RLO 1830.

[1] Grunwald, E.; Jumper, C. F.; Meiboom, S.; *J. Am. Chem. Soc.* **1963**, *85*, 522; Grunwald, E.; Meiboom, S.; *J. Am. Chem. Soc.* **1963**, *85*, 2047; Grunwald, E.; Jumper, C. F.; *J. Am. Chem. Soc.* **1963**, *85*, 2051; Luz, Z.; Meiboom, S.; *J. Am. Chem. Soc.* **1963**, *85*, 3923.
[2] Vinogradov, S. N.; Linnell, R. H.; *Hydrogen Bonding*; Van Nostrand Reinhold Co., New York, 1971; p. 217.
[3] Grunwald, E.; Eustace, D. in *Proton Transfer Reactions*, Caldin, E.; Gold, V; Ed.: Chapman and Hall, London, 1975; p. 103
[4] Bell, R. P.; Millington, J. P.; Park, J. M.; *Proc. Roy Soc. A* **1968**, *303*, 1; Bell, R. P.; Evans, P. G.; *Proc. Roy Soc. A* **1966**, *291*, 297.
[5] More O'Ferral, R. A.; *J. Chem. Soc. B* **1970**, 274.
[6] Hine, J.; *J. Am. Chem. Soc.* **1972**, *94*, 5766.
[7] Critchlow, J. E.; *J. Chem. Soc. Faraday Trans.***1972**, *68*, 1774.
[8] Hibbert, F.; *Adv. Phys. Organic Chem.* **1986**, *22*, 113, and references therein.
[9] Gandour, R. D.; Maggiora, G. M.; Schowen, R. L.; *J. Am. Chem. Soc.* **1974**, *96*, 6967.

[10] Williams, I. H.; Maggiora, G. M.; Schowen, R. L.; *J. Am. Chem. Soc.* **1980**, *102*, 7831; Williams, I. H.; Spangler, D.; Femec, D. A.; Maggiora, G. M.; Schowen, R. L.; *J. Am. Chem. Soc.* **1983**, *105*, 31; Williams, I. H.; *J. Am. Chem. Soc.* **1987**, *109*, 6299.

[11] Kong, Y. S.; Jhon, M. S.; Löwdin, P.; *I. J. Quant. Chem.* **1987**, *14*, 189.

[12] See for example, Hibbert, F. in *Comprehensive Chemical Kinetics*, Bamford, C. H.; Tipper, C. F. H., Ed.; Elsevier: New York, 1977; p. 97, and references therein.

[13] See for example, Crooks, J. E. in *Comprehensive Chemical Kinetics*, Bamford, C. H.; Tipper, C. F. H., Ed.; Elsevier: New York, 1977; p. 197, and references therein.

[14] Bell, R. P.; Critchlow, J. E.; *Proc. Roy. Soc. A* **1971**, *325*, 35.

[15] Isaacson, A. D.; Truhlar, D. G.; Rai, S. N.; Steckler, R.; Hancock, G. C.; Garrett, B. C.; Redmon, M. J. *Computer Phys. Comm.* **1987**, *47*, 91.

[16] Truhlar, D. G.; Garrett, B. C. *Acct. Chem. Res.* **1980**, *13*, 440.

[17] Walker, R. B.; Light, J. C. *Ann. Rev. Phys. Chem.* **1980**, *31*, 401.

[18] Pechukas, P. *Ann. Rev. Phys. Chem.* **1981**, *32*, 159.

[19] Truhlar, D. G.; Isaacson, A. D.; Skodje, R. T.; Garrett, B. C. *J. Phys. Chem.* **1982**, *86*, 2252; *J. Phys. Chem.* **1983**, *87*, 4554.

[20] Truhlar, D. G.; Hase, W. L.; Hynes, J. T. *J. Phys. Chem.* **1983**, *87*, 2664.

[21] Truhlar, D. G.; Garrett, B. C. *Ann. Rev. Phys. Chem.* **1984**, *35*, 159.

[22] Truhlar, D. G.; Isaacson, A. D.; Garrett, B. C. *The Theory of Chemical Reaction Rates*; Baer, M., Ed.; CRC Press: Boca Raton, FL, 1985; Vol. 4, p 65.

[23] For Version 1.1 see Ref. 9 ; For Version 1.5 see Isaacson, A. D.; Truhlar, D. G.; Rai, S. N.; Hancock, G. C.; Lauderdale, J. G.; Truong, T. N.; Joseph, T.; Garrett, B. C.; Steckler, R. *POLYRATE Program manual*, 1988.

[24] Garrett, B. C.; Truhlar, D. G. *J. Phys. Chem.* **1979**, *83*, 1079; *J. Phys. Chem.* **1983**, *87*, 4553.

[25] Garrett, B. C.; Truhlar, D. G.; Grev, R. S.; Magnuson, A. W. *J. Phys. Chem.* **1980**, *84*, 1730; *J. Phys. Chem.* **1983**, *87*, 4553.

[26] Glasstone, S.; Laidler, K. J.; Eyring, H.; *The Theory of Rate Processes*; McGraw-Hill: New York, 1941.

[27] Wigner, E. Z.; *Phys. Chem. B* **1932**, *19*, 203.

[28] Melius, C. F.; Binkley, J. S.; Paper WSS/CI 83-16, 1983 Fall Meeting of the Western States Section of the Combustion Institute, University of California, Los Angeles, Oct. 17-18, 1983.

[29] Melius, C. F.; Binkley, J. S. *The Chemistry of Combustion Processes* (ACS Symp. Ser. No. **249**); Sloane, T. M., Ed.; American Chemical Society: Washington, D.C., 1984; p 103.

[30] Melius, C. F.; Binkley, J. S.; *Symp. (Int.) Comb. [Proc.]* **1985**, *20*, 575.

[31] Perry, R. A.; Melius, C. F.; *Symp. (Int.) Comb. [Proc.]* **1985**, *20*, 639.

[32] Ho, P.; Coltrin, M. E.; Binkley, J. S.; Melius, C. F.; *J. Phys. Chem.* **1985**, *89*, 4647; *J. Phys. Chem.* **1986**, *90*, 3399.

[33] Garrett, B. C.; Koszykowski, M. L.; Melius, C. F.; Page, M.; *J. Phys. Chem.* **1990**, *94*, 7096.

[34] Bell, R. P.; *The Proton in Chemistry, 2nd Ed.*; Chapman and Hall, London, 1973.

[35] Lewis, E. S. in *Proton Transfer Reactions*, Caldin, E.; Gold, V; Eds: Chapman and Hall, London, 1975; p. 317

[36] Del Bene, J. E.; Kochenour, W. L.; *J. Am. Chem. Soc.* **1976**, *98*, 2041.

[37] Karlstrom, G.; Wennerstrom, H.; Jonsson, B.; Forsen, S.; Almlöf, J.; Roos, B.; *J. Am. Chem. Soc.* **1975**, *97*, 4188; Karlstrom, G.; Jonsson, B.; Roos, B. Wennerstrom, H.; *J. Am. Chem. Soc.* **1976**, *98*, 6851.

[38] Bouma, W. J.; Vincent, M. A.; Radom, L.; *Int J. Quantum Chem.* **1978**, *14*, 767.

[39] Bicerano, J.; Schaefer, H. F., III; Miller, W. H.; *J. Am. Chem. Soc.* **1983**, *105*, 2550.

[40] Baughcum, S. L.; Smith, Z.; Wilson, E. B.; Duerst, R. W.; *J. Am. Chem. Soc.* **1984**, *106*, 2260.

[41] *Gaussian 88*, Frisch, M. J.; Head-Gordon, M.; Schlegel, H. B.; Raghavachari, K.; Binkley, J. S.; Gonzalez, C.; Defrees, D. J.; Fox, D. J.; Whiteside, R. A.; Seeger, R.; Melius, C. F.; Baker, J.; Martin, R.; Kahn, L. R.; Stewart, J. J. P.; Fluder, E. M.; Topiol, S.; Pople, J. A.; Gaussian Inc., Pittsburgh, PA, **1988**.

[42] Krishnan, R.; Binkley, J. S.; Seeger, R.; Pople, J. A.; *J. Chem. Phys.* **1980**, *72*, 650.

[43] Page, M.; McIver, J. W., Jr.; *J. Chem. Phys.* **1988**, *88*, 922.

[44] Kendall, R. A.; private communication.

[45] Pople, J. A.; Binkley, J. S.; Seeger, R. *Int. J. Quantum Chem. Symp.* **1976**, *10*, 1; Pople, J. A.; Krishnan, R.; Schlegel, H. B.; Binkley, J. S.; *Int. J. Quantum Chem. Symp.* **1978**, *14*, 545.

[46] Skodje, R. T.; Truhlar, D. G.; Garrett, B. C.; *J. Chem. Phys.* **1982**, *77*, 5955.

[47] Skodje, R. T.; Truhlar, D. G.; Garrett, B. C.; *J. Phys. Chem.* **1981**, *85*, 3019.

[48] Miller, W. H.; Handy, N. C.; Adams, J. E.; *J. Chem. Phys.* **1980**, *72*, 99.

[49] Garrett, B. C.; Truhlar, D. G.; Wagner, A. F.; Dunning, T. H., Jr.; *J. Chem. Phys.* **1983**, *78*, 4400.

[50] Garrett, B. C.; Joseph, T.; Truong, T. N.; Truhlar, D. G.; *Chem. Phys.* **1989**, *136*, 271.

[51] Lauderdale, J. G.; Truhlar, D. G.; *J. Am. Chem. Soc.* **1985**, *107*, 4590; *Surf. Sci.* **1985**, *164*, 558; *J. Chem. Phys.* **1986**, *84*, 1843.

[52] Rice, B. M.; Garrett, B. C.; Koszykowski, M. L.; Foiles, S. M.; Daw, M. S.; *J. Chem. Phys.* **1990**, *92*, 775.

[53] Chase, M. W., Jr.; Davies, C. A.; Downey, J. R., Jr.; Frurip, D. J.; McDonald, R. A.; Syverud, A. N.; "JANAF Thermochemical Tables, 1985 Supplement" *J. Physical Chemical Reference Data* **1985**, *14*.

[54] Dyke, T. R.; Mack, K. M.; Muenter, J. S.; *J. Chem. Phys.* **1977**, *66*, 498.

[55] Curtiss, L. A.; Frurip, D. J.; Blander, H.; *J. Chem. Phys.* **1979**, *71*, 2703.

[56] Smith, E. J.; Swanton, D. J.; Pople, J. A.; Schaefer, H. F. III; Radom, L.; *J. Chem. Phys.* **1990**, *92*, 1240.

[57] Curtiss, L. A.; M. Blander, M.; *Chem. Rev.* **1988**, *88*, 827.

[58] Popkie, H.; Kistenmacher, H.; Clementi, E.; *J. Chem. Phys.* **1973**, *59*, 1325; Clementi, E.; Kolos, W.; Lie, G. C.;, Ranghino, G.; *Int. J. Quantum Chem.* **1980**, *17*, 377; Niesar, U.; Corongiu, G.; Huang, M.-J.; Dupuis, M.; Clementi, E.; *Int. J. Quantum Chem. Symp.* **1989**, *23*, 421.

[59] Chałasiński, G.; Szcześniak, M. M.; Cieplak, P.; Scheiner, S.; preprint.

[60] Melius, C. F.; Bergan, N.; Shepherd, J. E.; *Symp. (Int.) Comb. [Proc.]* **1990**, *23*, 0000.

END

DATE FILMED

02 / 05 / 91